Adjoint Moment Tensor Inversion for Non-Double Couple Earthquake: Synthetic Test

Azhar Harisandi[1,*], David Prambudi Sahara[1], Andri Hendriyana[1]

[1]Program Studi Teknik Geofisika FTTM Institut Teknologi Bandung
*Email: azharharisandi@gmail.com

Abstrak: Metode optimasi menggunakan *operator adjoint* dapat menjadi suatu solusi untuk menghitung turunan atau sensitivitas dari fungsi misfit terhadap parameter model. Dalam kasus pemodelan gelombang seismik dengan metode full-waveform, metode ini dapat dilakukan dengan menghitung interaksi antara gelombang dari hasil forward modeling dan gelombang adjoint yang dihasilkan dari mempropagasikan sumber adjoint ke dalam model bumi. Penerapan metode ini sudah ditunjukkan dalam beberapa literatur dalam kasus tomografi *full-waveform* dan inversi adjoint *full-waveform* untuk momen tensor. Pada penelitian ini, dilakukan eksperimen untuk melihat potensi dan stabilitas metode ini untuk melakukan inversi untuk gempa *non-double couple* dengan mendefinisikan beberapa kasus sintetik. Dari hasil tes sintetik yang dilakukan terlihat bahwa metode ini memiliki potensi untuk mencitrakan gempa non-double couple jika dilakukan tahap pengolahan awal untuk mengkoreksi efek ketidakakuratan struktur kecepatan. Hal ini dapat dilihat dari diperolehnya konvergensi menuju model referensi untuk kasus gempa non-DC walaupun model awal yang digunakan sama sekali tidak dekat dengan model referensinya. Jika tidak diterapkan, tahap pengolahan awal ini berefek pada konvergensi dan kemunculan noise numerik yaitu komponen *non-double couple* untuk gempa yang sebenarnya *double couple*.

Kata kunci: inversi *full-waveform*, metode adjoint, momen tensor

Abstract: *Adjoint method provides an elegant framework for computing the gradient of the misfit function with respect to model parameters. For the case of full-waveform adjoint moment tensor inversion, this can be achieved by recording the adjoint strain field in the source location. This adjoint strain is the product of adjoint simulation which can be achieved by solving the wave equation backwards in time from the receiver to the earth model and using waveform misfit as the adjoint source. In this paper, several test cases were defined to investigate the potential and stability of adjoint full-waveform inversion to invert moment tensor of non-DC earthquakes. The results from the test cases shows that misfit convergence to the reference model can be achieved if proper pre-processing step is applied to the waveform. Even for non-DC earthquake inversion that was using DC earthquake as a starting model. If this pre-processing step is not applied, this method can introduce a non-DC noise originating primarily from a non-accurate velocity structure and poor misfit*
convergence.

Keywords: adjoint method, full-waveform inversion, moment tensor

1 INTRODUCTION

Full-waveform seismic simulation nowadays has become more popular as computing power gets better at a more reasonable price. Also, this matter is supported by the development of spectral element method and open-source software that employs said method which can simulate the physics of wave equation for earth model with 3D varying velocity structure with great accuracy (Komatitsch et al., 1998; Komatitsch and Tromp, 1999). This advancement in simulating seismic wavefield give rise to an advancement in seismic ground motion simulation for earthquake monitoring using 3D varying earth model (Chodacki, 2020; Komatitsch et al., 2004; Gharti et al., 2017). Unfortunately, using full-waveform physics as forward model give rise to a very challenging problem in the optimization step, as we need to compute the gradient of the misfit function with respect to the model parameters to search for the optimum model. As the model parameters itself is very high dimensional, using brute-force method such as finite difference to compute the gradient of misfit function will become intractable (Fichtner, 2010). Adjoint method provides an elegant alternative in computing the gradient of the misfit function of full-waveform problem by taking the recorded wavefield and computing the interaction between the time-reversed wavefield with the simulated forward wavefield. This method then can be used as an optimization scheme for waveform tomography (e.g. Bozdağ et al., 2016; Liu and Tromp, 2006; Modrak and Tromp, 2016; Tromp et al., 2005; Tape et al., 2007, 2010) and moment tensor inversion. (Kim et al., 2011). Other variation of full-waveform inversion to invert moment tensor or source location also available in literature such as using time-reversal imaging or using pre-computed 3D Green's function and finite-difference based gradient-based optimization (e.g. Gharti et al., 2011; Kawakatsu and Montagner, 2008; Liu et al., 2004; Wang et al., 2020). In this research we are interested in examining the behaviour of adjoint method for inverting full moment tensor, specifically for micro-earthquake in mining activity. Because there is a high likelihood that an earthquake in the mining environment originating from anthropogenic source, the ability to

invert for the full moment tensor and its waveform becomes an interesting opportunity in this environment.

2   METHODOLOGY

2.1   Moment Tensor

Moment tensor is an object that contains information about contribution of each impulse response generated by a force couple to the total wavefield. For example, if we were to have a force couple with an arm in q-axis with force directing to the p-direction, the n-th component of a seismogram s located in x will be the convolution of the pq-th element of the moment tensor M_{pq} times the source-time function with the spatial derivative of the impulse response G_{np} in q direction (Eq. 1).

$$s_n(x,t) = M_{pq} * G_{np,q} \qquad (1)$$

The force couple is used because we must obey the conservation of linear and angular momentum in representing the body force equivalent of a fault-slip or other internal dislocation mechanism as there is no externally applied forces in that scenario (Aki and Richards, 2002; Backus and Mulcahy, 1976). In interpreting the moment tensor, we can decompose it into its component. One of the popular moment tensor decompositions is the decomposition into its double couple (DC), isotropic (ISO) and compensated linear vector dipole (CLVD) component (Jost and Herrmann, 1989). These components are interpreted to represent other mechanism of non-tectonic earthquake, such as explosion, or crack openings.

2.2   Adjoint Wavefield and Misfit Functional

When defining an optimization problem, we will later have to come up with a function that measures the goodness of fit of our forward model synthetic compared to the observed data. In full-waveform inversion, one of the most intuitive misfit functions is the windowed squared difference between the synthetic $s(x_r, t; m)$ and observed waveform $d(x_r, t)$ (Eq. 2). Where $w_r p(t)$ represents a windowing function for receiver r and component r. The dependency of the synthetic to the model that is being used in generating that synthetic is expressed explicitly in the m symbol in $s(x_r, t; m)$, and x_r refers to the position of one receiver. As defined by Kim et al. (2011), if we use waveform misfit as our misfit function χ and computing the variation of the misfit function while ignoring the variations due to structural parameter, we arrived at the definition of the adjoint wave equation along with the adjoint source in Eq. 3. Where c is the elasticity tensor for the earth model, $\ddot{s}^\dagger$ is the adjoint displacement field, and ρ is the density of the earth model. As we can see that the adjoint source itself is the time-reversed and windowed waveform difference.

$$\chi = \frac{1}{2} \sum_{rp} \int W_{rp}(t) \, ||\mathbf{s}(x_r, t; \mathbf{m}) - \mathbf{d}(x_r, t)||^2 \, dt \qquad (2)$$

$$\rho \ddot{s}^\dagger = \nabla.(c : \nabla \ddot{s}^\dagger) + \sum_{rp} [W_{rp}(s - \mathbf{d})] (T - 2t_0 - t) \, \delta(x - x_r) \qquad (3)$$

Taking the partial derivatives with respect to moment tensor element we then will get the Fréchet derivative of the misfit functional (Eq. 4). This equation shows how we can compute the derivative of the misfit function with respect to the moment tensor element by convolving adjoint strain field $\epsilon_{ij}^\dagger$ with source time function S in the source location x_s. This gradient can later be used in any gradient-based optimization scheme.

2.3   Nonlinear Conjugate-Gradient Method

In this study, we use non-linear conjugate gradient method with Polak-Ribiere scheme and periodic reset as an optimization algorithm (Eq. 4), as this scheme has shown to have an advantage by resetting the constant when computing the descent direction (Eq. 5) (Shewchuk, 1994). Where $\hat{p}^k$ is the vector pointing to descent direction for k-th iteration, $\hat{g}^k$ is the gradient of the misfit functional for the k-th iteration, and $\hat{\beta}^k$ governs how much does the previous gradient iteration contribute to the current iteration.

$$\hat{p}^k = -\hat{g}^k + \hat{\beta}^k \hat{p}^{k-1} \qquad (4)$$

$$\hat{\beta}^k = \max\left(0, \frac{\hat{g}^k. \left(\hat{g}^k - \hat{g}^{k-1}\right)}{\hat{g}^{k-1}.\hat{g}^{k-1}}\right) \qquad (5)$$

3   SYNTHETIC TEST CASES

In this research, we defined several scenarios to test adjoint method to invert for non-DC earthquake. We only tested the inversion for the moment tensor element without updating the location or the source-time function. First, we wanted to test whether a DC earthquake will still be inverted as a DC earthquake if we use DC model as a starting model. In investigating the behaviour of this algorithm for DC earthquake, we made two scenarios, one without waveform cross-correlation to correct for the effect of incorrect velocity structure and the other one corrected using cross-correlation and time shift (Komatitsch et al., 2004; Liu et al., 2004). Later we defined four other scenarios, each to test the behaviour of this algorithm for pure implosion, explosion, and CLVD earthquake as a target/reference model with the same DC moment tensor as the starting model. To simulate the effect of incorrect velocity variation, we use the reference velocity model (Figure 1a) to simulate the target/reference waveform and use the oversmoothed version of the velocity model (Figure 1b) to be used in inversion. For non-DC earthquake test cases, we employ optimization with waveform cross-correlation and time shift as pre-processing before computing adjoint source. As this pre-processing method gives more desirable result shown later in the DC to DC inversion. All the scenarios used in this research is summarized in Table 1.

4   RESULT AND DISCUSSION
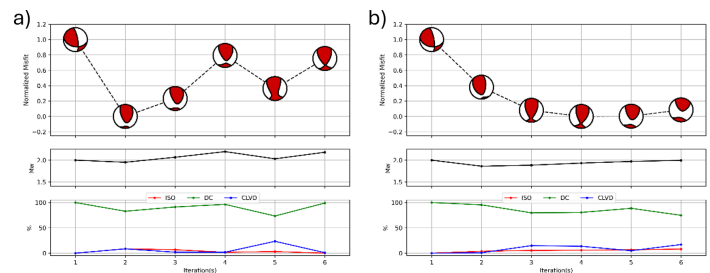
4.1   DC to DC inversion

For scenario 1, the misfit convergence is relatively poor, shown by the fluctuations of the misfit evolution plot in Figure 2a, but the algorithm can already give a reasonable model
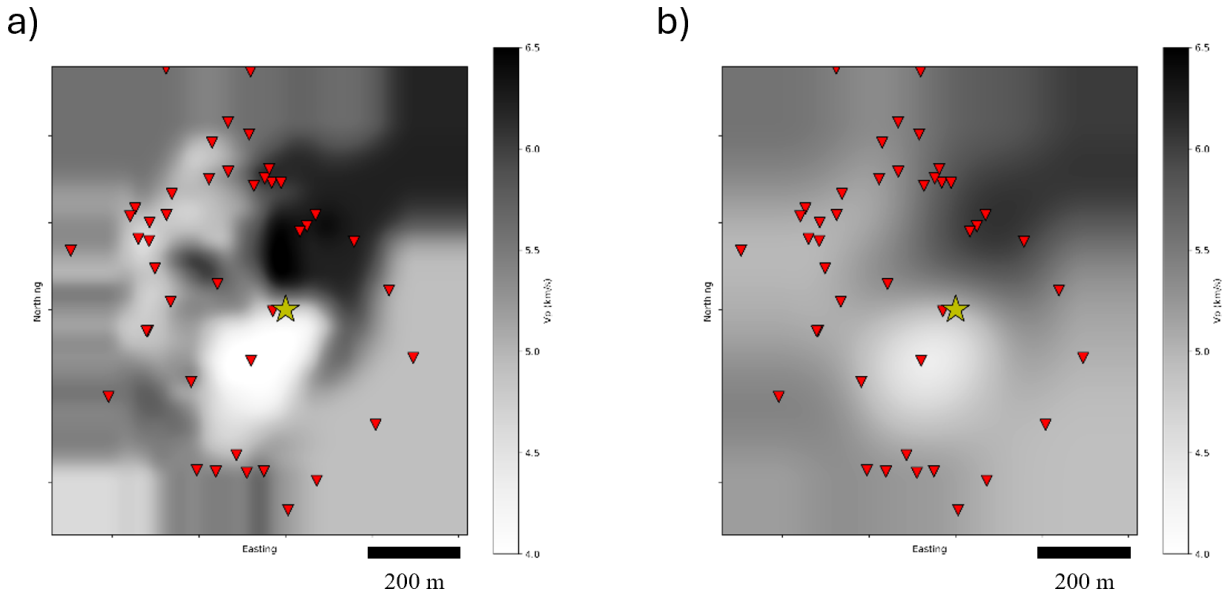
Figure 1. Z-slice of true velocity model used for generating synthetic data (a) and smoothed version to be used in inversion (b). Yellow star represents the synthetic earthquake location used in this study and red reversed triangles showing the stations distribution

Table 1. Summary of synthetic scenarios

Scenario	Starting MT Model	Target/ True MT Model	Cross-correlation & Time Shift
1			No
2			Yes
3			Yes
4			Yes
5			Yes
6			Yes

Figure 2. Misfit, beachball plot, magnitude, and ISO, DC, & CLVD component evolution for each iteration for scenario 1 (a) and scenario 2 (b)

Table 2. Summary of inverted DC parameters for scenario 1

	Starting MT	Best MT	Target MT
Mw	2	1.95	2
Strike 1/ Strike 2	100.00/ 350.34	31.97/ 153.81	43.99/ 150.00
Dip 1/ Dip 2	40.00/ 74.24	63.37/ 43.54	52.84/ 70.00
Rake 1/ Rake 2	25.00/ 127.25	139.41/ 54.18	154.59/ 40.00

in the second iteration. Whereas in the scenario 2 the misfit convergence is better and can give the best model (model with the smallest misfit in the entire iteration) but needed 4 iterations to give the best model. If we look at the full moment tensor in Table 2 and Table 3, the one without velocity structure correction (scenario 1) returns a moment tensor with a greater non-DC noise. But this non-DC component is relatively negligible in percentage (< 15 %). As for the moment magnitude, fault plane orientation and rake, both gives a reasonable estimate without deviating significantly from the true value with scenario 2 performing better than scenario 1.

[b]

Table 3. Summary of inverted DC parameters for scenario 2

|	Starting MT	Best MT	Target MT
Mw	2	1.93	2
Strike 1/ Strike 2	100.00/ 350.34	41.65/ 155.09	43.99/ 150.00
Dip 1/ Dip 2	40.00/ 74.24	53.56/ 61.68	52.84/ 70.00
Rake 1/ Rake 2	25.00/ 127.25	143.87/ 42.43	154.59/ 40.00

4.2 DC to non-DC inversion

The result from inverting non-DC earthquake using DC moment tensor as a starting model gives a surprisingly good result, as we can see in the Figure 3 that final model resembles the target model nearly in a perfect way and the component of target percentage rises approximately 50% from starting model. For example, in scenario 3, as the target model is isotropic (explosion), our starting model has zero isotropic component, but in the final model the isotropic component increases to nearly 50%.

One thing that interesting in the misfit evolution plot is that the moment magnitude fluctuates quite significantly, especially for the pure isotropic model (explosion and implosion), the best model yields a very accurate beachball pattern compared to the reference target model, but the magnitude decreases significantly. For the isotropic case it may be that it requires more iterations to converge to a reasonable estimate of magnitude. This observation shows that this method can potentially invert for non-DC earthquake, but we have to keep in mind that this is a controlled noiseless experiment. Other effect has to be taken into account for further studies such as updating the location, or even the effect of velocity anisotropy in the earth model. The other thing that must be considered is the threshold of the ISO, DC and CLVD percentage. In this case, it is difficult to quantify the uncertainty of those components as sampling method would require a considerable amount of time and computing power as the forward modeling step alone is already expensive to execute.

5 CONCLUSION

We have demonstrated that adjoint moment tensor inversion has a promising potential to invert the full moment tensor for a non-DC earthquake. As shown from the experiment, for DC to DC earthquake, this algorithm gives a model that resembles perfectly the target model given that essential pre-processing step is applied to the waveform. For non-DC earthquake this method also gives a remarkably good result, given that we use a significantly different starting model compared to the target model. This is of course only a synthetic case, but from this synthetic case we can already see that this tool will still provide a valuable insight about
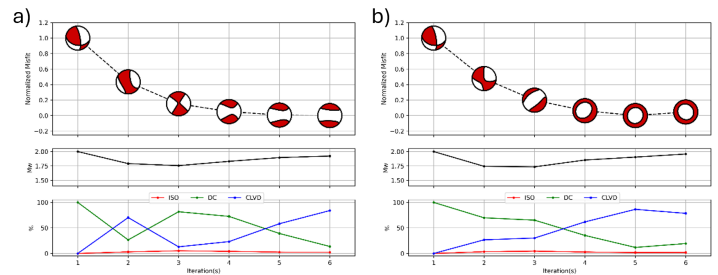
Figure 3. Misfit, beachball plot, magnitude, and ISO, DC, & CLVD component evolution for each iteration for scenario 3 (a), scenario 4 (b), scenario 5 (c) and scenario 6 (c)
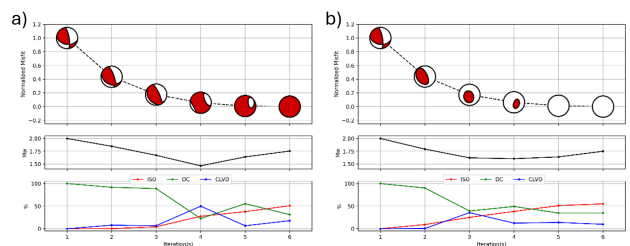
Figure 4. Misfit, beachball plot, magnitude, and ISO, DC, & CLVD component evolution for each iteration for scenario 5 (a) and scenario 6 (b)

seismicity beneath our earth model. Given that we have a 3D velocity structure and point source, we can simulate the wavefield and optimize it to study our source model at that given time.

References

Aki, K. and Richards, P.G. (2002): Quantitative Seismology. University Science Books, 2nd edn., ISBN 0935702962.

Backus, G. and Mulcahy, M. (1976): Moment tensors and other phenomenological descriptions of seismic sources—i. continuous displacements. *Geophysical Journal of the Royal Astronomical Society*, **46**(2), 341–361, doi:https://doi.org/10.1111/j.1365-246X.1976.tb04162.x.

Bozdağ, E. et al. (2016): Global adjoint tomography: first-generation model. *Geophysical Journal International*, **207**(3), 1739–1766, ISSN 0956-540X, doi:10.1093/gji/ggw356.

Chodacki, J. (2020): Simulation of ground motion in a polish coal mine using spectral-element method. *Journal of Seismology*, **24**, 363–373, ISSN 1573-157X, doi:10.1007/s10950-020-09911-w.

Fichtner, A. (2010): Full Seismic Waveform Modelling and Inversion. Advances in Geophysical and Environmental Mechanics and Mathematics, Springer Berlin Heidelberg, ISBN 9783642158070, doi:https://doi.org/10.1007/978-3-642-15807-0.

Gharti, H., Oye, V., Kühn, D. and Zhao, P. (2011): Simultaneous microearthquake location and moment-tensor estimation using time-reversal imaging. *SEG Te-*

chnical Program Expanded Abstracts 2011, 1632–1637, doi:10.1190/1.3627516.

Gharti, H., Oye, V., Roth, M. and Kühn, D. (2017): Wave propagation modelling in various microearthquake environments using a spectral-element method. *arXiv physics.geo-ph*, doi:10.48550/arXiv.1706.05217.

Jost, M.L. and Herrmann, R.B. (1989): A Student's Guide to and Review of Moment Tensors. *Seismological Research Letters*, **60**(2), 37–57, ISSN 0895-0695, doi:10.1785/gssrl.60.2.37.

Kawakatsu, H. and Montagner, J.P. (2008): Time-reversal seismic-source imaging and moment-tensor inversion. *Geophysical Journal International*, **175**(2), 686–688, ISSN 0956-540X, doi:10.1111/j.1365-246X.2008.03926.x.

Kim, Y.H., Liu, Q. and Tromp, J. (2011): Adjoint centroid-moment tensor inversions. *Geophysical Journal International*, **186**(1), 264–278, ISSN 0956-540X, doi:10.1111/j.1365-246X.2011.05027.x.

Komatitsch, D., Liu, Q., Tromp, J., Suss, P., Stidham, C. and Shaw, J.H. (2004): Simulations of Ground Motion in the Los Angeles Basin Based upon the Spectral-Element Method. *Bulletin of the Seismological Society of America*, **94**(1), 187–206, ISSN 0037-1106, doi:10.1785/0120030077.

Komatitsch, D. and Tromp, J. (1999): Introduction to the spectral element method for three-dimensional seismic wave propagation. *Geophysical Journal International*, **139**(3), 806–822, ISSN 0956-540X, doi:10.1046/j.1365-246x.1999.00967.x.

Komatitsch, D., Tromp, J. and Vilotte, J. (1998): The spectral element method for elastic wave equations: Application to 2D and 3D seismic problems. 1460–1463, doi:10.1190/1.1820185.

Liu, Q., Polet, J., Komatitsch, D. and Tromp, J. (2004): Spectral-Element Moment Tensor Inversions for Earthquakes in Southern California. *Bulletin of the Seismological Society of America*, **94**(5), 1748–1761, ISSN 0037-1106, doi:10.1785/012004038.

Liu, Q. and Tromp, J. (2006): Finite-frequency kernels based on adjoint methods. *Bulletin of the Seismological Society of America*, **96**(6), 2383–2397, ISSN 0037-1106, doi:10.1785/0120060041.

Modrak, R. and Tromp, J. (2016): Seismic waveform inversion best practices: regional, global and exploration test cases. *Geophysical Journal International*, **206**(3), 1864–1889, ISSN 0956-540X, doi:10.1093/gji/ggw202.

Shewchuk, J.R. (1994): An introduction to the conjugate gradient method without the agonizing pain. *Carnegie-Mellon University. Department of Computer Science.*

Tape, C., Liu, Q., Maggi, A. and Tromp, J. (2010): Seismic tomography of the southern California crust based on spectral-element and adjoint methods. *Geophysical Journal International*, **180**(1), 433–462, ISSN 0956-540X, doi:10.1111/j.1365-246X.2009.04429.x.

Tape, C., Liu, Q. and Tromp, J. (2007): Finite-frequency tomography using adjoint methods—Methodology and examples using membrane surface waves. *Geophysical Journal International*, **168**(3), 1105–1129, ISSN 0956-540X, doi:10.1111/j.1365-246X.2006.03191.x.

Tromp, J., Tape, C. and Liu, Q. (2005): Seismic tomography, adjoint methods, time reversal and banana-doughnut kernels. *Geophysical Journal International*, **160**(1), 195–216, ISSN 0956-540X, doi:10.1111/j.1365-246X.2004.02453.x.

Wang, Y., Shang, X., Wang, Z. and Gao, R. (2020): High-accuracy location of microseismic events in a strong inhomogeneous mining environment by optimized global full waveform inversion. *Applied Sciences*, **10**(20), ISSN 2076-3417, doi:10.3390/app10207205.